Hindawi Publishing Corporation
International Journal of Rotating Machinery
Volume 2007, Article ID 51598, 8 pages
doi:10.1155/2007/51598

Research Article

Effect of Blade Profile on the Performance of Wells Turbine under Unidirectional Sinusoidal and Real Sea Flow Conditions

A. Thakker and R. Abdulhadi

Wave Energy Research Team, Department of Mechanical and Aeronautical Engineering, University of Limerick, L1-011 Limerick, Ireland

Received 25 January 2007; Accepted 2 November 2007

Recommended by Ken-Ichiro Takeishi

This paper presents the effect of blade profile and rotor solidity on the performance of Wells turbine operating under unidirectional unsteady flow conditions. In the study, four kinds of blade profile were selected, that is, NACA0020, NACA0015, CA9, and HSIM 15-262123-1576. The experiments have been carried out for two solidities, $\sigma = 0.48$ and $\sigma = 0.64$, under sinusoidal and irregular unsteady flow conditions based on Irish waves (site2). As a result, it was found that the preferable rotor geometry is the one with blade profile of CA9 with solidity $\sigma = 0.64$. In addition, the effect of blade profile and rotor solidity on hysteretic characteristics of the turbine has been clarified experimentally and it was found to be in good agreement qualitatively when compared to numerical results (Setoguchi et al. (2003)).

1. INTRODUCTION

Over the last few decades, scientists have been investigating and defining different methods for power extraction from wave motion. The most successful and most extensively studied device for power extraction energy from ocean waves is the oscillating water column (OWC) device. The OWC-based wave energy power plants convert wave energy into low-pressure pneumatic power in the form of bidirectional airflow. Self-rectifying air turbines are used to extract mechanical shift power. Two different turbines are currently in use around the world for wave energy power generation, the Wells turbine, introduced by Dr A.A Wells (Raghunathan [1]) in 1976, and impulse turbine by some authors (Kim et al. [2]; Setoguchi et al. [3]). Both these turbines are currently in operation in different power plants in Europe, India, Japan, Korea, and so forth. The research around the world is focused on improving the performance of both these turbines under different operating conditions.

The present investigation deals with the Wells turbine. There are many reports, which describe the performance of the Wells turbine both at starting and running characteristics (Gato et al. [4]; Inoue et al. [5, 6]; Raghunathan et al. [7]). According to these results, the Wells turbine has inherent disadvantages—lower efficiency, poor starting, and higher noise level in comparison to conventional turbines (Kim et al. [8]; Takao et al. [9]). In order to enhance the performance of the Wells turbine, some rotor blade profiles of Wells turbine have been tested under steady inlet flow condition. It has been found by Setoguchi et al. [10] that the optimum blade profile for small-scale Wells turbine such as the navigation buoy (Setoguchi and Takao [11]) (i.e., the turbine operated at low Reynolds number) is NACA0020. On the other hand, for large-scale Wells turbine, which is installed in wave energy power plant such as LIMPT system (Boake et al. [12]; Renewable Energy World [13]), Islay, UK (i.e., the turbine is operated at high Reynolds number), it has been found by Takao et al. [14] that the optimum blade profile is NACA0015. Furthermore, the effects of blade profile under sinusoidal and real sea flow conditions have not been clarified yet.

The objective of this study is to clarify the effect of blade profile and solidity on the performance of large-scale Wells turbine under various inlet flow conditions such as sinusoidal and real sea conditions. In this study, blade profiles tested experimentally on 0.6 m Wells turbine were

Table 1: Specification of turbines.

Airfoil	Thickness ratio	Maximum thickness Position (x/l)	Solidity at mean radius σ_r (number of rotor blades z)	Remarks 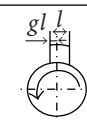
NACA0020	0.2	0.3	0.48(6), 0.64(8)	Rotor diameter = 597 mm Hub-to-tip ratio ν = 0.6 Tip clearance = 1 mm Chord length l = 120 mm Aspect ratio = 1 Sweep ratio g = 0.5
NACA0015	0.15	0.3		
CA9	0.15	0.198		
HSIM15-262123-1576	0.15	0.1576		

NACA0020, NACA0015, CA9, and HSIM 15-262123-1576 (this is named HSIM15 in the following discussion) for two solidities σ = 0.48 and σ = 0.64. Also, the hysteretic characteristics of Wells turbine operating under various inlet flow conditions and various rotor geometry has been tested experimentally.

2. ROTOR BLADE PROFILE FOR WELLS TURBINE

In 1976, the Wells turbine was proposed as a form of self-rectifying axial flow air turbine which is suitable for wave energy conversion in OWC. In order to enhance the performance of the Wells turbine to determine the optimum turbine geometry, various researches have been conducted studies and published papers in relation to the rotor blade profile for the Wells turbine. According to previous studies, symmetrical airfoil of NACA four digit series is preferable one, especially it has been shown that the NACA four digit series with thickness ratio of approximately 20% is recommended one for the rotor blade (Raghunathan [1]; Setoguchi et al. [10]). On the other hand, CA9 and HSIM15 were proposed recently as newly devised blades in order to delay the onset of separation and postpone the blade stall (Thakker et al. [15]; Webster and Gato [16]). The aim of development of the optimized blades is to extend the operation range of the Wells turbine. The profiles of these blades are shown together with NACA0020 and NACA0015 in Figure 1. Both the new blades were optimized in terms of leading edge radius, maximum thickness position, and trailing edge slope, so as to improve the pressure distribution around the airfoil. This is because the separation on the adverse pressure gradient. As is evident from the figure, the maximum thickness position of two optimized blades is moved toward the leading edge in comparison with NACA0020 and NACA0015. The positions of NACA blade, CA9, and HSIM15 are x/l = 0.3, 0.198, and 0.1576, respectively. Furthermore, when compared with NACA0015, radius of the leading edge of two optimized blades is enlarged. Particularly, the radius of HSIM15 is almost the same to that of NACA0020.

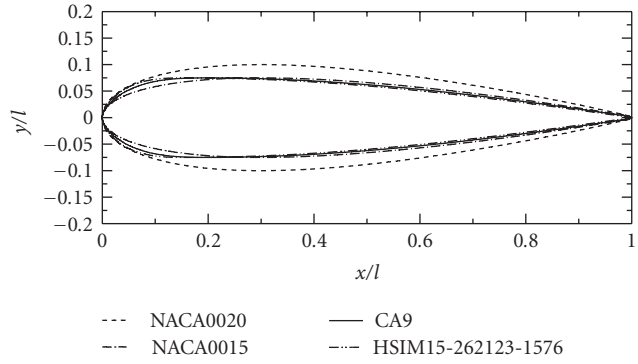

Figure 1: Blade profile.

3. EXPERIMENTAL SETUP

A schematic layout of the experimental setup of Wave Energy Research Team, University of Limerick, is shown in Figure 2. It consists of a bell mouth entry, test section, drive and transmission section, a plenum chamber with honeycomb section, a calibrated nozzle, and a centrifugal fan. Air is drawn into the bell mouth-shaped open end; it passes through the turbine and then enters the plenum chamber. In the chamber, the flow is conditioned and all swirls/vortices are removed prior to passing through a calibrated nozzle and finally exhausting at the fan outlet. A valve at fan exit controls the flow rate. The turbine test section had an internal diameter of 600 mm and fabricated rotor and a diameter of 598 mm, leaving tip clearance of 1 mm. The hub diameter is selected as 358.8 mm, providing hub to tip ratio of 0.6. The turbine was mounted on a shaft in a cylindrical annular duct. The shaft is coupled to motor/generator via a torque meter. The turbine blades (8 blades for σ = 0.64 and 6 blades for σ = 0.48) were set on the hub at a 90° angle of stagger along the y-axis.

In the study, four kinds of symmetrical blade profile with chord length l of 120 mm were used for the experiments. The blade profile and the turbine specification are shown in Table 1. The blade profiles were investigated for two solidities

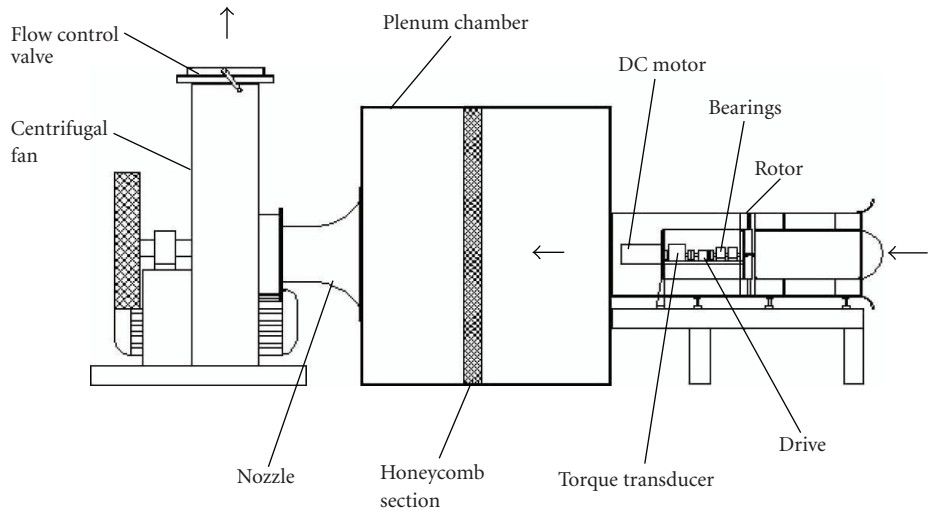

Figure 2: Schematic diagram of test rig.

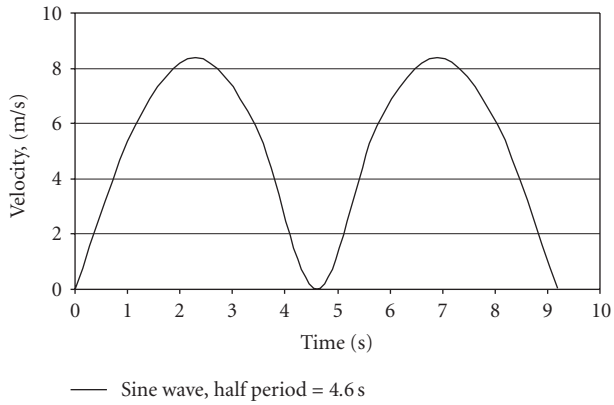

Figure 3: Variation of inlet velocity with time for sine waves with half period of 4.6 seconds.

($\sigma = 0.48$ and $\sigma = 0.64$). The experiments were carried out for NACA0020, NACA0015, CA9, and HSIM15 blade profile.

4. EXPERIMENTAL PROCEDURE

The sinusoidal and random (Irish Sea Climate) wave inlet conditions to the turbine have been generated by controlling the open area of centrifugal fan outlet of test rig using a valve actuator. Initially, the valve actuator was calibrated to find the correlation between the open area of fan exit and pressure drop across the nozzle (ΔP_n) at inlet to the fan. Later, the relation between the valve displacement and flow rate through the test section was arrived using the nozzle calibration curve. In order to generate a given regular or random wave, time history of valve displacement was calculated using the above mentioned method. The valve actuator controller was utilized to operate the valve according to the time history. For this purpose, a computer program has been written (Ryan [17]) and controller was interfaced with a computer.

The procedure involves fixing the rotor at a set speed and generating the required flow pattern (Sinusoidal flow or site2 conditions). Performance parameters were recorded using a high-speed logger that is part of the data acquisition system (Thakker et al. [18]).

The overall performance of the turbine was evaluated by the turbine angular velocity ω, torque generated T, flow rate Q, and total pressure drop across the rotor ΔP_r. The results are expressed in the form of torque coefficient C_T, input power coefficient C_A, efficiency η, and mean average efficiency η_t. The definitions are given below:

$$C_T = \frac{T}{\rho * \omega^2 * r_t^5}, \tag{1}$$

$$C_A = \frac{\Delta P_r * Q}{\rho * \omega^2 * r_t^2}, \tag{2}$$

$$\eta = \frac{T * \omega}{\Delta P_r * Q}, \tag{3}$$

$$\phi = \frac{v_a}{Ut}, \tag{4}$$

$$\eta_t = \frac{\sum [T * \omega]}{\sum [\Delta P * Q]}. \tag{5}$$

5. RESULT AND DISCUSSION

5.1. Effect of rotor geometry on turbine characteristic under various inlet flow conditions

Since the airflow into the turbine is generated by the OWC, it is very important to clarify the turbine characteristics under oscillating inlet flow conditions. Initially the performance test of the turbine has been conducted with sinusoidal inlet flow condition. As mentioned earlier, the test rig used for this purpose was unidirectional and hence only half upper portion of the sine wave was generated. Later, the experiments

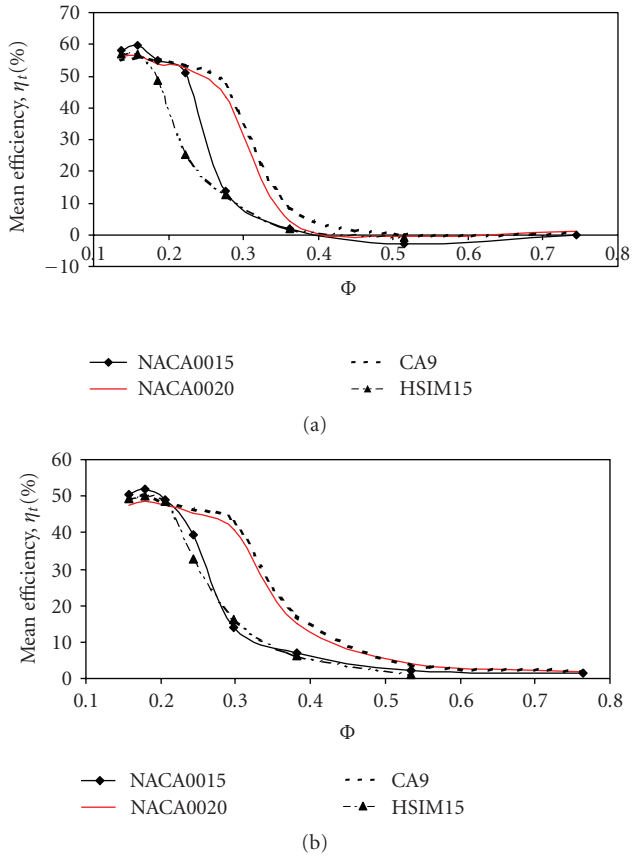

Figure 4: Effect of blade profile on mean efficiency under sinusoidal flow conditions: (a) $\sigma = 0.48$, (b) $\sigma = 0.64$.

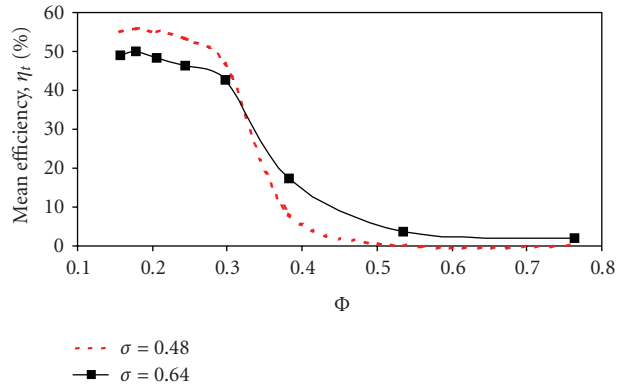

Figure 5: Effect of rotor solidity on the mean efficiency of CA9 under sinusoidal flow conditions.

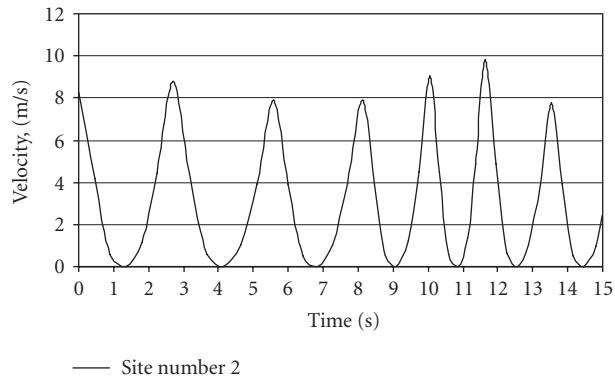

Figure 6: Variation of inlet velocity with time of Irish Sea condition (site2).

have been conducted with unsteady and irregular inlet flow condition of an Irish Sea wave conditions (site2). The Irish wave data was provided by Electricity Supply Board International (ESBI), Ireland.

5.2. Effect of blade profile and rotor solidity on turbine characteristics under regular sinusoidal inlet flow

Experiments have been conducted on four different blade profiles of Wells turbine, that is, NACA0020, NACA0015, CA9, and HSIM15 operating under inlet flow conditions, based on sine wave with half period of 4.6 seconds, Figure (3).The peak velocity of the sine wave was kept constant at 8.9 m/s. Figures 4(a) and 4(b) illustrate the effect of blade profile on mean efficiency under sinusoidal flow conditions for two solidities ($\sigma = 0.48$ and $\sigma = 0.64$), respectively. The mean efficiencies were calculated from the time-averaged instantaneous input and torque flow coefficient (5). It was found from the figures for both solidity that the highest mean efficiency is obtained for the case of turbine with NACA0015 at value of flow coefficient $\Phi = 0.17$. Conversely, at high flow coefficient $\Phi > 0.24$, the mean efficiency for NACA0015 is observed to be lower than NACA0020 and CA9 and the operation range is narrow. Regarding HSIM15, the mean efficiency is relatively high at low coefficient $\Phi < 0.2$; however, the operation range of this blade profile is the narrowest in all cases. This is because of the Reynolds number effect (Takao et al. [14]). With respect to NACA0020 and CA9, Figures 4(a) and 4(b) show that the stall characteristic of CA9 blade profile is the best in all cases; consequently, the power extracted from the CA9 blade profile is the highest. Furthermore, Figure (5) shows the effect of rotor solidity on the mean efficiency of CA9. It is clear from the figure that the highest mean efficiency was obtained for the turbine with solidity $\sigma = 0.48$; however, beyond stall point, the turbine with solidity $\sigma = 0.48$ has lower mean efficiency than that with solidity $\sigma = 0.64$.

5.3. Effect of blade profile and rotor solidity on turbine characteristics under real sea inlet flow condition

Experiments have been conducted on four different blade profiles of Wells turbine, that is, NACA0020, NACA0015, CA9, and HSIM15 operating under irregular and random inlet flow conditions based on Irish Sea climate (site2). The variation of inlet velocity with time for sites2 is shown in Figure (6). The average of half-time periods of site2 is 4.6 seconds.

Figures 7(a) and 7(b) show the effect of blade profile on the mean efficiency of Wells turbine under real sea condition site2 for two different solidities $\sigma = 0.48$, $\sigma = 0.64$,

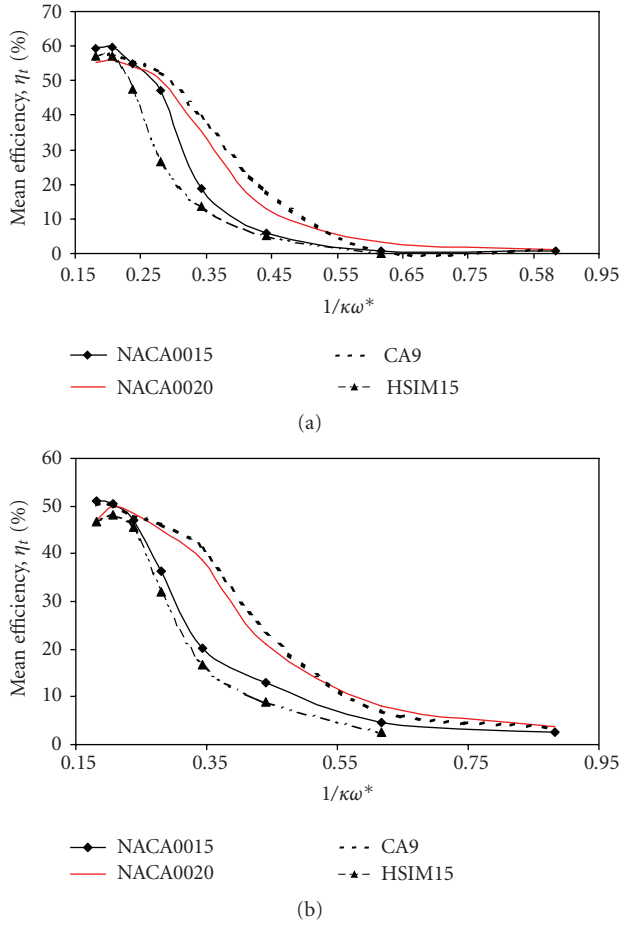

FIGURE 7: Effect of blade profile on the mean efficiency under real sea conditions (site2): (a) $\sigma = 0.48$, (b) $\sigma = 0.64$.

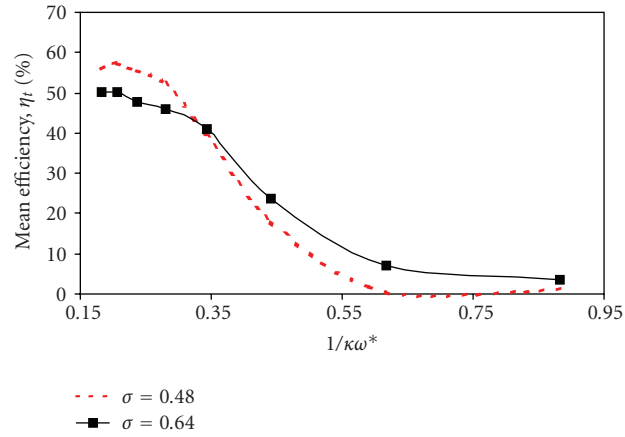

FIGURE 8: Effect of rotor solidity on the mean efficiency of CA9 under real sea conditions (site2).

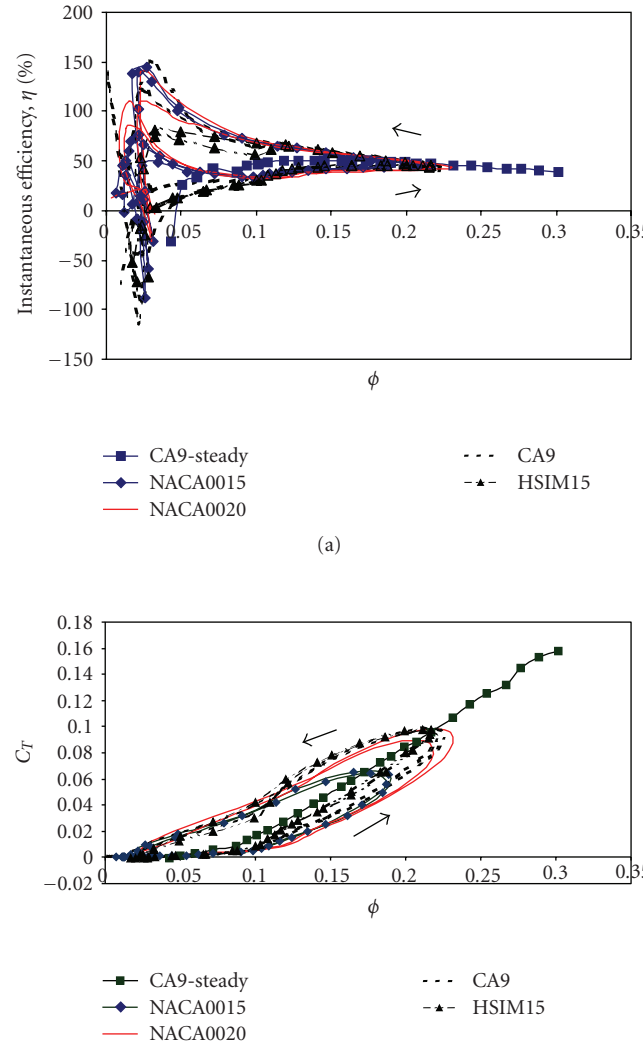

FIGURE 9: Variations of instantaneous efficiency and torque coefficient for different blade profile at $1/\kappa\omega^* = 0.2$ ($\sigma = 0.64$): (a) efficiency, (b) torque coefficient.

respectively. Similar to the case of sinusoidal inlet flow conditions; in the random and irregular flow conditions the operation range for the turbine with CA9 is wider than other turbines. This means that the Reynolds number has less effect on the performance of CA9 blade profile comparison to other blades profile. It was observed that the operation range of HSIM15 is the narrowest in the all blades.

Figure (8) shows the effect of rotor solidity on the mean efficiency of CA9. It is found from the figure that before stall point the mean efficiency of the turbine $\sigma = 0.48$ is higher than that $\sigma = 0.64$. Conversely, beyond stall point, the mean efficiency of $\sigma = 0.48$ becomes low in comparison with $\sigma = 0.64$. In comparison with the case of sinusoidal flow condition, similar performance trend was seen for both site2 and sinusoidal flow conditions.

6. STUDY ON THE INSTANTANEOUS RESULTS

In order to analysis the difference in behavior of Wells turbine at lower and higher $1/\kappa\omega^*$ values, instantaneous efficiency and torque coefficient have been plotted for a number of half periods of site2 condition. Figures 9(a) and 9(b) show the instantaneous efficiency and torque coefficient of NACA0020, NACA0015, CA9, and HSIM15 for $\sigma = 0.64$, at

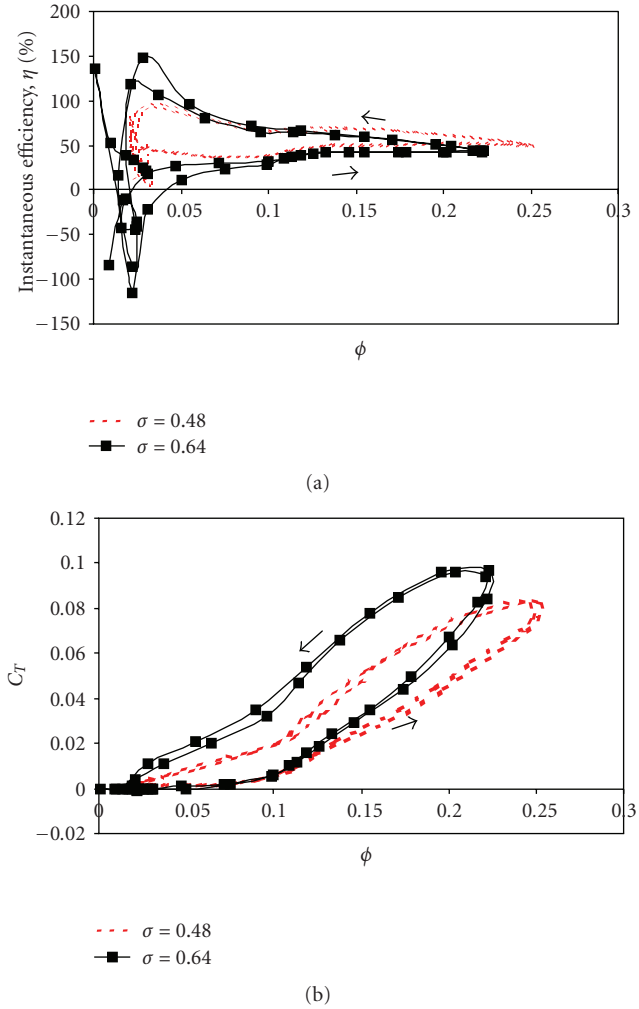

Figure 10: Variation of instantaneous efficiency and torque coefficient of CA9 with $\sigma = 0.48$ and $\sigma = 0.64$ at value $1/\kappa\omega^* = 0.2$: (a) efficiency, (b) torque coefficient.

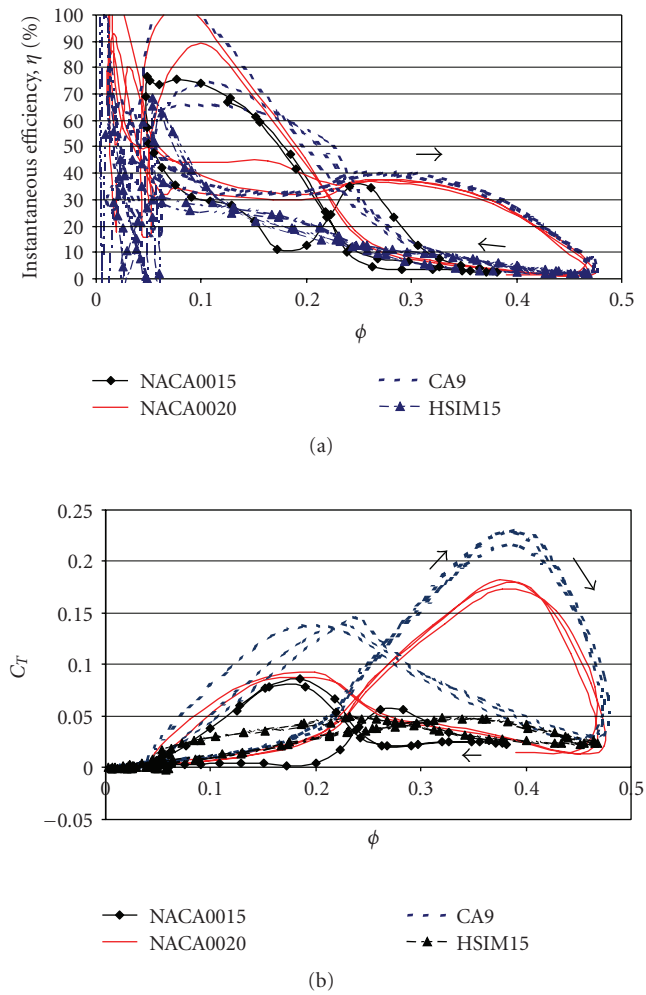

Figure 11: Variations of instantaneous efficiency and torque for different blade profile coefficient at $1/\kappa\omega^* = 0.44$ ($\sigma = 0.64$): (a) efficiency, (b) torque coefficient.

low value of flow coefficient ($1/\kappa\omega^* = 0.2$). The nondimensional term $1/\kappa\omega^*$ represents the flow coefficient for ordinary fluid machines. The parameter $\kappa\omega^*$ includes characteristic parameters of the irregular waves (H_s and T_s), turbine speed (ω), and dimensions of the turbine and air chamber (rt and m). The turbine characteristics of CA9 blade profile under steady flow conditions [14] have been plotted for comparison. From the figures, the efficiency and the torque coefficient follow two different paths. During acceleration of inlet flow, the velocity goes from zero to maximum value, and during deceleration of inlet flow, the velocity goes from maximum to zero velocity. Also it forms a counter clockwise hysteretic loop per half period of wave. Furthermore, as can be seen from the figures, during the acceleration, the curves obtained from random testing follow a similar trend to those obtained during steady state testing. However, the steady state efficiency curves fail to present the rapid rise in efficiency during deceleration, which occurs at low flow coefficient ϕ. The spike in efficiency that occurs at the low flow coefficient may be considered as follows. When the flow approaches minimum value the rotor has energy stored in it, in the form of inertia, therefore a positive torque is being recorded resulting in a high instantaneous efficiency. In addition, when the torque become negative, the efficiency drops off dramatically to negative values until the flow begins to accelerate again.

Figures 10(a) and 10(b) show the effect of rotor solidity on the instantaneous efficiency and torque coefficient of CA9 blade profile of Wells turbine. Figure 10(a) shows that the instantaneous efficiency of $\sigma = 0.48$ is higher than that of $\sigma = 0.64$ during acceleration and deceleration. On the other hand, it is obvious from Figure 10(b) that the instantaneous torque coefficient developed by $\sigma = 0.64$ is higher than that developed by $\sigma = 0.48$ during acceleration and deceleration. Figures 11(a) and 11(b) illustrate the variations of efficiency and torque coefficient of NACA0020, NACA0015, CA9, and HSIM15 blade profiles at high value of flow coefficient ($1/\kappa\omega^* = 0.44$), for $\sigma = 0.64$, respectively. As is evident from the figures, the variation of instantaneous efficiency and torque coefficient indicates a clockwise loop due

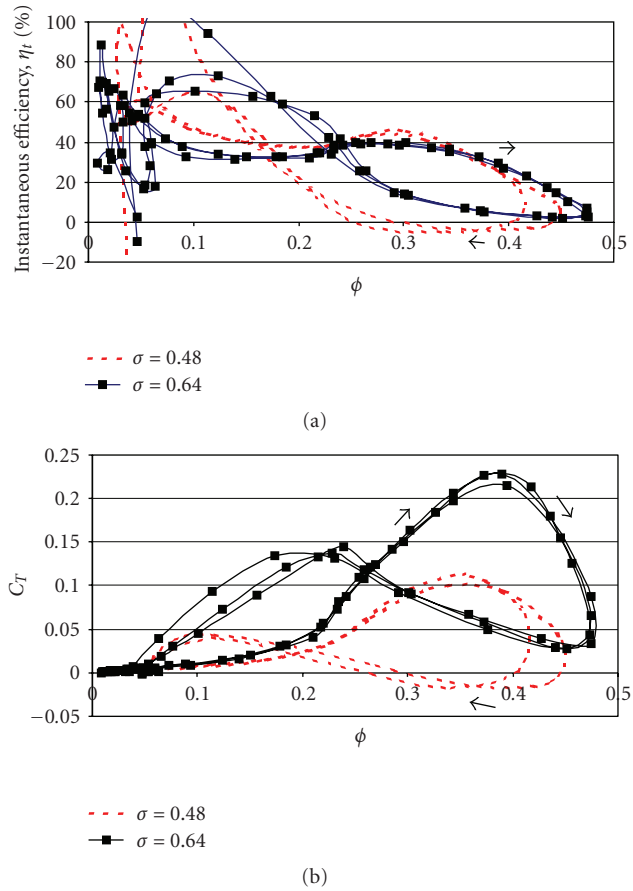

FIGURE 12: Variation of instantaneous efficiency and torque coefficient of CA9 with $\sigma = 0.48$ and $\sigma = 0.64$ at value $1/\kappa\omega^* = 0.44$: (a) efficiency, (b) torque coefficient.

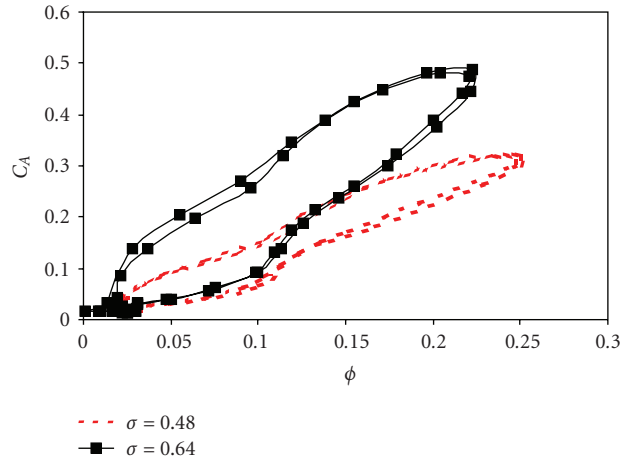

FIGURE 13: Effect of solidities on the hysteretic characteristics of CA9 under real sea conditions (site2) at $1/\kappa\omega^* = 0.2$, $\sigma = 0.64$.

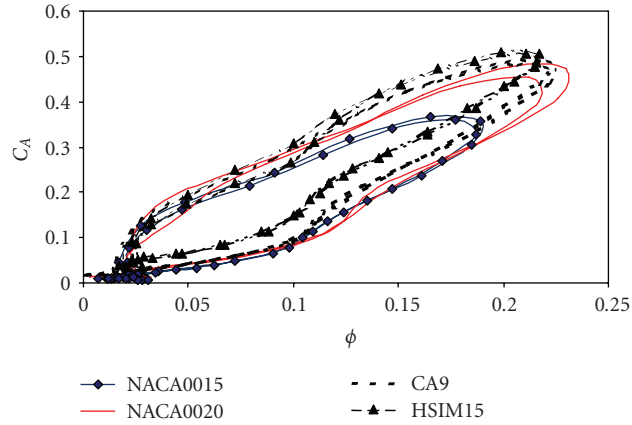

FIGURE 14: Effect of blade profile on the hysteretic characteristics of Wells turbine under real sea conditions (site2) at $1\kappa\omega^* = 0.18$, $\sigma = 0.64$.

to the dynamic stall. In addition, the torque coefficient and stall point of CA9 are far superior in all cases. Regarding NACA0020, although the efficiency and torque coefficient are lower than those of CA9, the stall point and the efficiency are higher than those of NACA0015 and HSIM15. One could see also that HSIM15 has a very low efficiency comparison with other turbines.

Figures 12(a) and 12(b) show the effect of rotor solidity on the instantaneous efficiency and torque coefficient for CA9. One could see form the figures that, during the acceleration of inlet flow, although the maximum instantaneous efficiency of $\sigma = 0.48$ is higher than that of $\sigma = 0.64$, the torque coefficient of $\sigma = 0.64$ is higher than that of $\sigma = 0.48$. On the other hand, the instantaneous efficiency and torque coefficient of $\sigma = 0.64$ are higher than that of $\sigma = 0.48$ during the deceleration of inlet flow. Furthermore, beyond stall point, the torque coefficient value of $\sigma = 0.48$ is negative during the deceleration in comparison to the positive value of $\sigma = 0.64$. Therefore, it seems that the turbine with $\sigma = 0.48$ has poor starting characteristics.

In order to investigate the effect of rotor solidity and blade profile on hysteretic characteristics. The C_A curve was used for this purpose. Figure (13) shows the effect of rotor solidity on the hysteretic behavior of CA9 Wells turbine at low value of $1/(\kappa\omega^*)$. It is clear from the figure that the size of the hysteretic loop of C_A decreases significantly with the decrease in rotor solidity. Furthermore, the C_A values of $\sigma = 0.48$ is less than $\sigma = 0.64$. This drop in input coefficient explains the reduction in efficiency for $\sigma = 0.64$. Figure (14) shows the effect of blade profile on the hysteretic behavior of the Wells turbine for ($\sigma = 0.64$). It is apparent from the figure that the hysteretic characteristics of the Wells turbine is less sensitive to the blade profile. Moreover, the experimental result of hysteretic characteristics was in good agreement compare to the numerical results (Setoguchi et al. [19]).

7. CONCLUSIONS

In order to clarify the effect of blade profile on the performance of 0.6 m Wells turbine for wave energy conversion, four kinds of blade profile were selected, that is, NACA0020, NACA0015, CA9, and HSIM15. The experimental investigations have been performed for two Wells turbine solidities $\sigma = 0.48$ and $\sigma = 0.64$, operating under sinusoidal and real sea conditions (site2). It was observed from the experimental

results that although the maximum mean efficiency was achieved for NACA0015 turbine in comparison to CA9 turbine, its operation range was narrower to that of CA9. As a result, it has been concluded that the preferable rotor geometry is the blade profile of CA9. Furthermore, at low flow coefficient, for all blade profiles, it was found that the maximum mean efficiency of turbine with $\sigma = 0.48$ is far superior to that of $\sigma = 0.64$. However, the trend is reverse at high flow coefficient. It is important to note that the turbine with $\sigma = 0.48$ has poor starting characteristics, therefore it was concluded that the preferable rotor solidity is $\sigma = 0.64$.

It was also found that the experimental results based on the turbine operating under reciprocating flow showed similar trends to that of steady flow results during the acceleration. However, the steady flow efficiency curve fails to present the rapid rise in efficiency during deceleration, which occurred at low flow coefficient.

The effect of blade profile and rotor solidity on the hysteretic behavior of wells turbine have been clarified experimentally, and it was in good agreement qualitatively when compared to the numerical results (Setoguchi et al. [19]).

SYMBOLS

H_s: Significant wave height
k: Nondimensional period $((r_t\ m)/H_s)$
l: Chord length of rotor blade
m: Turbine to OWC open area ratio
r_t: Tip span radius
T_s: Mean period of incident wave
U_t: Circumferential velocity at r_t
v_a: Axial flow velocity
V_a: Maximum value of v_a
ϕ: Flow coefficient
Φ: Flow coefficient under sinusoidal flow (V_a/U_t)
ρ: Density of air
σ: Rotor solidity

REFERENCES

[1] S. Raghunathan, "Performance of the Wells self-rectifying turbine," *The Aeronautical Journal*, vol. 89, no. 1368, pp. 369–379, 1985.

[2] T. W. Kim, K. Kaneko, T. Setoguchi, and M. Inoue, "Aerodynamic performance of an impulse turbine with self-pitch-controlled guide vanes for wave power conversion," in *Proceedings of the 1st KSME-JSME Thermal and Fluids Engineering Conference*, vol. 2, pp. 133–137, Seoul, Korea, July 1988.

[3] T. Setoguchi, M. Takao, Y. Kinoue, K. Kaneko, S. Santhakumar, and M. Inoue, "Study on an impulse turbine for wave energy conversion," *International Journal of Offshore and Polar Engineering*, vol. 10, no. 2, pp. 145–152, 2000.

[4] L. M. C. Gato, V. Warfield, and A. Thakker, "Performance of a high-solidity wells turbine for an OWC wave power plant," *Journal of Energy Resources Technology*, vol. 118, no. 4, pp. 263–268, 1996.

[5] I. Inou, K. Kaneko, S. Setoguchi, and S. Raghunathan, "Simulation of starting characteristics of the Wells turbine for wave power generator," in *Proceedings of the 4th AIAA/ASME Fluid Mechanics, Plasma Dynamics and Lasers Conference*, Atlanta, Ga, USA, 1986, AIAA-86-1122.

[6] I. Inou, K. Kaneko, S. Setoguchi, and S. Shimamoto, "Studies on Wells turbine for wave power generator," *Bulletin of the JSME*, vol. 29, no. 250, pp. 1177–1182, 1986.

[7] S. Raghunathan, T. Setoguchi, and K. Kaneko, "Wells air turbine subjected to inlet flow distortion and high levels of turbulence," *International Journal of Heat and Fluid Flow*, vol. 8, no. 2, pp. 165–167, 1987.

[8] T.-H. Kim, M. Takao, T. Setoguchi, K. Kaneko, and M. Inoue, "Performance comparison of turbines for wave power conversion," *International Journal of Thermal Sciences*, vol. 40, no. 7, pp. 681–689, 2001.

[9] M. Takao, T. Setoguchi, K. Kaneko, S. Raghunathan, and M. Inoue, "Noise characteristics of turbines for wave power conversion," *Journal of Power and Energy*, vol. 216, no. 3, pp. 223–228, 2002.

[10] T. Setoguchi, M. Takao, K. Itakura, M. Mohammad, K. Kaneko, and A. Thakker, "Effect of rotor geometry on the performance of Wells turbine," in *Proceedings of the 13th International Offshore and Polar Engineering Conference (ISOPE '03)*, vol. 1, pp. 345–350, Honolulu, Hawaii, USA, May 2003.

[11] T. Setoguchi and M. Takao, "State of art on self-rectifying air turbines for wave energy conversion," in *Proceedings of the 4th International Conference on Mechanical Engineering*, pp. 117–126, Dhaka, Bangladesh, 2001.

[12] C. B. Boake, T. J. T. Whittaker, M. Folley, and H. Ellen, "Overview and initial operational experience of the LIMPET wave energy plant," in *Proceedings of the 12th International Offshore and Polar Engineering Conference (ISOPE '02)*, vol. 12, pp. 586–594, Kitakyushu, Japan, May 2002.

[13] "Renewable Energy World," January-February 2001.

[14] M. Takao, A. Thakker, R. Abdulhadi, and T. Setoguchi, "Effect of blade profile on the performance of large-scale Wells turbine," in *Proceedings of the 14th International Offshore and Polar Engineering Conference (ISOPE '04)*, pp. 272–276, Toulon, France, May 2004.

[15] A. Thakker, P. Frawley, E. S. Bajeet, and A. Heffernan, "Experimental investigation of CA9 blades on a 0.3 m wells turbine rig," in *Proceedings of the 10th International Offshore and Polar Engineering Conference (ISOPE '00)*, vol. 1, pp. 345–350, Seattle, Wash, USA, May-June 2000.

[16] M. Webster and L. M. C. Gato, "The effect of rotor blade shape on the performance of the wells turbine," *International Journal of Offshore and Polar Engineering*, vol. 11, no. 3, pp. 227–230, 2001.

[17] J. Ryan, "Experimental analysis of irregular unsteady flow on performance of impulse turbine for wave energy conversion," M.Eng Thesis, University of Limerick, Limerick, Ireland, 2005.

[18] A. Thakker, T. S. Dhanasekaran, and J. Ryan, "Experimental studies on effect of guide vane shape on performance of impulse turbine for wave energy conversion," *Renewable Energy*, vol. 30, no. 15, pp. 2203–2219, 2005.

[19] T. Setoguchi, Y. Kinoue, T. H. Kim, K. Kaneko, and M. Inoue, "Hysteretic characteristics of Wells turbine for wave power conversion," *Renewable Energy*, vol. 28, no. 13, pp. 2113–2127, 2003.